



**HAL**  
open science

## Fluorescence correction for activity measurement of $^{93}\text{mNb}$ in niobium dosimeters: calculation and experimental validation

Marie-Christine Lépy, Jonathan Riffaud, Christophe Domergue, Herve Philibert, Christophe Destouches, Hubert Carcreff

### ► To cite this version:

Marie-Christine Lépy, Jonathan Riffaud, Christophe Domergue, Herve Philibert, Christophe Destouches, et al.. Fluorescence correction for activity measurement of  $^{93}\text{mNb}$  in niobium dosimeters: calculation and experimental validation. 17th International Symposium on Reactor Dosimetry (ISR D 2023), May 2023, Lausanne, Switzerland. 01001 (9 p.), 10.1051/epjconf/202327801001 . cea-04122563

**HAL Id: cea-04122563**

**<https://cea.hal.science/cea-04122563v1>**

Submitted on 8 Jun 2023

**HAL** is a multi-disciplinary open access archive for the deposit and dissemination of scientific research documents, whether they are published or not. The documents may come from teaching and research institutions in France or abroad, or from public or private research centers.

L'archive ouverte pluridisciplinaire **HAL**, est destinée au dépôt et à la diffusion de documents scientifiques de niveau recherche, publiés ou non, émanant des établissements d'enseignement et de recherche français ou étrangers, des laboratoires publics ou privés.



Distributed under a Creative Commons Attribution 4.0 International License

# Fluorescence correction for activity measurement of $^{93m}\text{Nb}$ in niobium dosimeters: calculation and experimental validation

Marie-Christine Lépy<sup>1\*</sup>, Jonathan Riffaud<sup>1</sup>, Christophe Domergue<sup>2</sup>, Hervé Philibert<sup>2</sup>, Christophe Destouches<sup>2</sup>, and Hubert Carcreff<sup>3</sup>

<sup>1</sup>Université Paris-Saclay, CEA, LIST, Laboratoire National Henri Becquerel (LNE-LNHB), 91120 Palaiseau, France

<sup>2</sup>CEA, DES/IRENE/DER/SPESI, Laboratoire de Dosimétrie, Capteurs et Instrumentation (LDCI), Cadarache, 13108 Saint Paul-lez-Durance, France

<sup>3</sup>Université Paris-Saclay, CEA, ISAS/DM2S, Service d'études des réacteurs et de mathématiques appliquées, 91191 Gif-sur-Yvette cedex, France

**Abstract.** Niobium is a dosimeter used to characterize fast-neutron reaction rates to monitor nuclear reactor vessels. Its characterization is based on the activity of  $^{93m}\text{Nb}$  resulting from the  $^{93}\text{Nb}(n,n')$  activation reaction. The decay of  $^{93m}\text{Nb}$  results mainly in the emission of niobium K X-rays which are used to determine the activity of  $^{93m}\text{Nb}$ . Direct measurement using X-ray spectrometry does not require any sample preparation, but fluorescence effects, due to impurities which are activated during irradiation, must be taken into account. Indeed, some of these radioactive impurities, in particular  $^{182}\text{Ta}$ , and other niobium isotopes remain present during the measurements and disturb the X-ray spectra. The fluorescence effect induces additional niobium X-ray emission to that due to the  $^{93m}\text{Nb}$  decay alone, which leads to an overestimation of the dosimeter activity, especially if the results are expected shortly after the end of the irradiation. It is therefore necessary to assess the contribution of fluorescence effects to provide accurate values of  $^{93m}\text{Nb}$  activity. Fluorescence correction factors were established by Monte Carlo simulation. The calculated fluorescence correction factors were validated by an experimental approach, using activated niobium dosimeters with different tantalum concentrations.

## 1 Introduction

Niobium is a dosimeter used to characterize fast-neutron reaction rates to monitor neutron damage to nuclear reactor vessels [1]. Its characterization is based on the activity of  $^{93m}\text{Nb}$  resulting from the activation reaction  $^{93}\text{Nb}(n, n')$ .  $^{93m}\text{Nb}$  is a metastable state of  $^{93}\text{Nb}$  that de-excites towards the ground state by an isomeric transition with a strong internal conversion coefficient. This decay results mainly in emission of niobium K X-rays which are used to determine the activity of  $^{93m}\text{Nb}$ , either by direct measurement using X-ray spectrometry or,

---

\* Corresponding author : [marie-christine.lepy@cea.fr](mailto:marie-christine.lepy@cea.fr)

after sample dissolution, using X-ray counting or liquid scintillation measurement. The first method does not require any sample preparation, but fluorescence effects can disturb the measurement, since niobium foils may contain impurities that are activated during irradiation. Some of these radioactive impurities, especially  $^{182}\text{Ta}$ , and other isotopes of niobium ( $^{94}\text{Nb}$ ,  $^{95}\text{Nb}$  and  $^{92\text{m}}\text{Nb}$ ) are still present during spectrometry measurements and disturb the X-ray spectra. The fluorescence effect generates additional niobium X-rays to those due only to the decay of  $^{93\text{m}}\text{Nb}$ , thus inducing an overestimation of the dosimeter activity. Most of the activated impurities have a much shorter half-life than that of  $^{93\text{m}}\text{Nb}$  and the current method consists in letting the dosimeters decay for several months, or even years if one considers the half-life of  $^{182}\text{Ta}$  (114 days), before proceeding with the measurement to provide a relevant activity. However, in some circumstances, results are expected much earlier, no long after the end of irradiation. It is therefore necessary to take into account the effects of fluorescence to provide accurate values of the activity of  $^{93\text{m}}\text{Nb}$ . The present study focuses on fluorescence corrective factors with a two-steps approach. First, the correction factors were established by Monte Carlo simulation. Second, these were validated by experimental measurements of niobium dosimeters with different tantalum levels that were submitted to an intense neutron flux. These dosimeters were measured six times throughout the year following the end of irradiation using gamma- and X-ray spectrometry to determine respectively the activity of the impurities and the niobium K X-rays emission rates. These rates were corrected for the impurities contribution using the calculated corrective factors before deriving the activity of  $^{93\text{m}}\text{Nb}$  at the same reference date.

## 2 Niobium dosimeters preparation and measurement

### 2.1 Niobium activation

Different reactions occur during neutron activation of niobium dosimeters and two kinds of radionuclides are produced. These result directly from the activation of niobium (Fig. 1) since, in addition to the reaction of interest ( $n, n'$ ), other processes such as ( $n, 2n$ ), ( $n, \gamma$ ) or ( $n, p$ ) can provide  $^{92}\text{Nb}$  and  $^{92\text{m}}\text{Nb}$ ,  $^{94}\text{Nb}$  and  $^{93}\text{Zr}$ , respectively. Moreover, in its natural state, niobium is usually found mixed with various other metals, notably tantalum. These are also activated and produce additional radionuclides, e.g.  $^{182}\text{Ta}$  is produced by radiative capture from  $^{181}\text{Ta}$ . Table 1 shows the main characteristics of the gamma-emitting impurities.

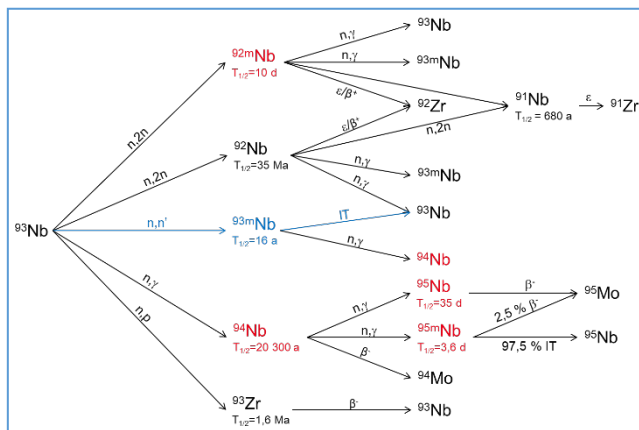


**Fig. 1.** Activation products from niobium-93

As the presence of tantalum leads to significant corrective factors, for this exercise it was chosen to work with different levels of tantalum impurity concentration. Nine niobium dosimeters with different Ta impurity levels, namely 0.3 ppm, 4 ppm and 19.6 ppm were activated in the MARIA reactor (National Centre for Nuclear Research, Poland) within the framework of the round robin initiated by the European Working Group on Reactor Dosimetry (EWGRD) [2]. The dosimeters were available as strips or discs, with the following characteristics: strips: thickness 20  $\mu\text{m}$ , length 5 mm, width 1 mm, mass 1 mg; discs: thickness 20  $\mu\text{m}$ , diameter 8 mm, mass 8.6 mg.

**Table 1.** Main characteristics of  $^{93\text{m}}\text{Nb}$  and of gamma-emitting impurities

Radionuclide	Half-life	Energy (keV)	Emission intensity (%)	Reference
$^{93\text{m}}\text{Nb}$	16.12 (15) a	16.58	9.66 (17)	DDEP – KRI 2013 [4]
		18.67	1.89 (4)	
$^{92\text{m}}\text{Nb}$	10.15 (2) d	934.44	99.07 (4)	NDS 66 – 1999 [3]
$^{94}\text{Nb}$	20.0 (24) $10^3$ a	702.62	97.9 (20)	NDS 44 & 66 - 1999[3]
		871.09	99.9 (1)	
$^{95}\text{Nb}$	34.991 (6) d	765.80	99.808 (7)	DDEP – INEL 2002[4]
$^{95\text{m}}\text{Nb}$	3.61 (3) d	235.69	25.1 (3)	DDEP – LPRI-INEL 202[4]
$^{182}\text{Ta}$	114.61 (13) d	1 121.29	35.17 (33)	DDEP – LNHB 2011[4]
		1 221.39	27.27 (27)	
$^{183}\text{Ta}$	5.1 (1) d	246.06	27.2	NDS [3]

## 2.2 Gamma spectrometry

Gamma spectrometry was used to quantify the activity of radioactive impurities. The spectrometer is based on an N-type high-purity germanium (HPGe) detector whose full-energy peak efficiency has been accurately determined using radioactive standards. A spectrum example is shown in Fig. 2 where the regions corresponding to impurities appear in red. The activity calculation is derived from the full-energy peaks corresponding to the characteristic energies shown in Table 1.

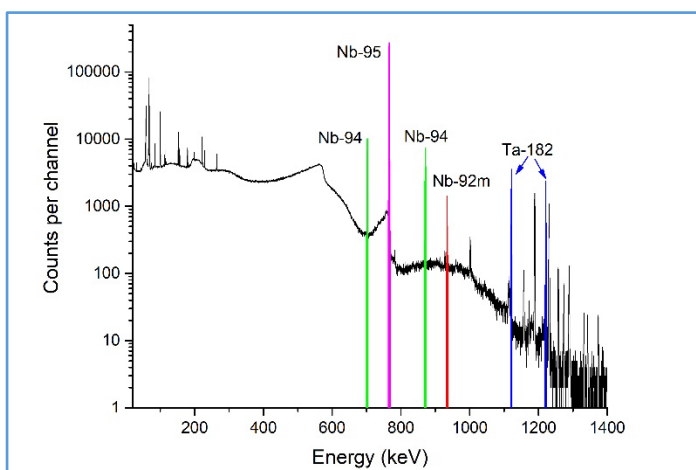


**Fig. 2.** Gamma spectrum in the 15 keV-1500 keV region allowing the quantification of impurities

The activity,  $A$  (Bq), of each radionuclide is calculated from the net area of the full-energy peaks corresponding to the energies of interest,  $N(E)$ , the acquisition time,  $t$  (s) (active time), the associated photon emission intensity,  $I(E)$  (see Table 1), the full-energy peak efficiency for the energy  $E$ ,  $\varepsilon(E)$ , and various corrective factors,  $C_i$ . These include radioactive decay, coincidence summing and self-attenuation [5].

$$A = \frac{N(E) \cdot \prod C_i}{\varepsilon(E) \cdot I(E) \cdot t} \quad (1)$$

### 2.3 X-ray spectrometry

X-ray spectrometry measurements were carried out with a spectrometer built around an N-type HPGe detector, adapted to low energies and equipped with two collimators to reduce scattering effects. As for the gamma-ray spectrometer, the full-energy peak efficiency has been accurately determined using radioactive standards. Fig. 3 illustrates the detailed processing of the region of interest which includes the peaks corresponding to K X-rays of niobium (16.6 keV and 18.7 keV) and zirconium (15.8 keV and 17.7 keV) as well as the  $K\alpha$  peak of molybdenum (17.4 keV). The peak areas are obtained using the COLEGRAM software [6] by fitting peak functions to the experimental points. Each peak is represented by a Voigt function, i.e. the convolution of a Lorentzian, which allows for the natural width of the X-ray lines, with a Gaussian, which reproduces the broadening of the detection process. The activity of each dosimeter is calculated with Eq. 1 for each niobium peak and the final result is the weighted mean of the two values. Due to the low energies considered, the self-attenuation correction factors, of an order of magnitude of 10 %, were computed by using the software ETNA [7]. In addition, corrective factors had to be calculated to take into account additional fluorescence induced by impurities (see §2.4).

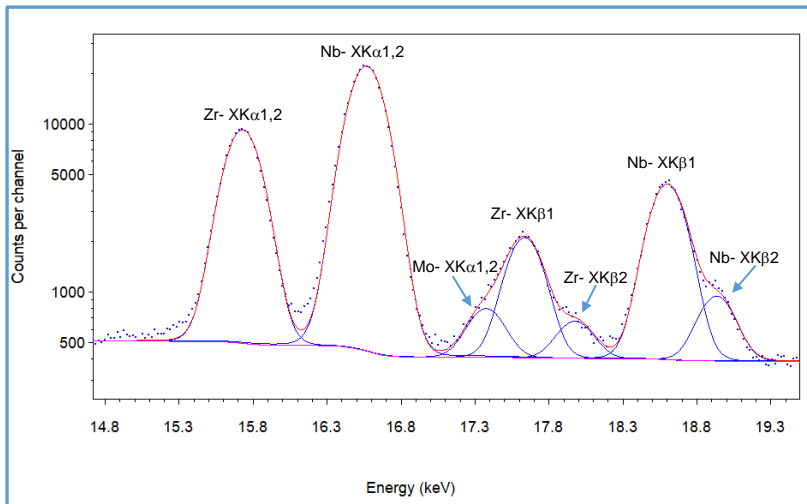


**Fig. 3.** Processing of the X-ray energy region of interest using COLEGRAM software

### 2.4 Fluorescence corrections

The main difficulty encountered in post-irradiation measurements is the presence of both niobium radioisotopes and the impurities in the dosimeter material, such as tantalum, which induce niobium fluorescence and contribute to increase counts in the niobium X-ray peaks.

### 2.4.1 Impurities main characteristics

Niobium-92m decays by electron capture and beta plus emission to the excited levels of zirconium-92; consequently, it also emits K X-rays of zirconium which are well identified in the spectra (see e.g. Fig. 3).

Niobium-94 and niobium-95 decay by beta minus emission to the excited levels of molybdenum-94 and molybdenum-95, respectively. Both provide K X-rays of molybdenum that are well separated from the niobium ones in the X-ray spectra. The molybdenum  $XK\beta$  emission (19.62 keV) being just above the niobium K ionization threshold (18.98 keV), it has a high probability of photoelectric interaction in the dosimeter material and thus of generating niobium fluorescence. However, the low intensity of Mo K X-ray emissions (about 0.2 % and 0.01 % for  $^{94}\text{Nb}$  and  $^{95}\text{Nb}$  respectively) limits their effect.

Niobium-95m decays mainly (97.5 %) by gamma transition to the niobium-95 ground level and 2.5 % by beta minus emission to the excited levels of molybdenum-95. It is characterized by its gamma emission at 235.69 keV (25.1 %) and K X-rays of niobium following electronic rearrangement after ejection of conversion electrons. Tantalum-182 decays by beta minus emission to the thirteen excited levels of tungsten-182. These rearrange in about 40 gamma transitions, with energies between 32 keV and 1453 keV. At low energy, one notes an intense gamma emission at 67.75 keV (43.6 %) and the K X-rays of tungsten at 58.8 keV and 67.7 keV, with respective intensities of 27 % and 7 %.

The decay scheme of  $^{183}\text{Ta}$  is similar to that of  $^{182}\text{Ta}$ , decaying by beta minus emission to eleven excited levels of tungsten-183, which give about 30 gamma transitions. The gamma energies are below 406 keV, the main ones being 246 keV and 354 keV with intensities of 27 % and 11.2 % respectively; the intensities of the K X-ray emissions from tungsten being of the order of 68 % for  $XK\alpha$  and 18 % for  $XK\beta$ .

### 2.4.2 Fluorescence effect on X-ray spectra

Any photon radiation from the decay of radioactive impurities with an energy above the K-binding energy of niobium can interact by photoelectric effect in the atomic K shell of the dosimeter material. The atomic relaxation following photoionisation leads to the emission of K X-rays of niobium. These induced fluorescence photons are detected in the same way as the K X-rays characteristic of  $^{93\text{m}}\text{Nb}$  decay, with the same energies and therefore contribute to increasing the areas of the full-energy peaks recorded in the spectra. It is therefore necessary to calculate factors to correct for this effect. This problem was studied in the doctoral work of Jonathan Riffaud [8] where the fluorescence induced by each impurity was simulated by Monte Carlo method in order to determine the different corrective factors.

## 3 Monte Carlo simulations

The fluorescence contribution from radionuclide  $N$  is obtained by simulating its radioactive decay in a niobium dosimeter, thus inducing the fluorescence of this material. This requires simulating the complete decay scheme of each radionuclide, taking into account interactions of the emitted particles with matter and atomic relaxation processes, using the PENNUC decay data file [9] from the Decay Data Evaluation Project (DDEP). The radioactive impurity was isotropically distributed inside the dosimeter and the simulation was performed under the geometrical measurement conditions of the X-ray spectrometer. The information collected corresponds to the energy deposited in the detector with the information of the process responsible for the niobium ionization. The simulated spectra include the characteristic peaks of the simulated radionuclide and the induced fluorescence peaks. Most

of the correction factors for fluorescence were established by Monte Carlo simulation using GEANT4 [10]. In addition, the correction factor for  $^{183}\text{Ta}$  was calculated with the PENELOPE 2018 code [11]. An example of the simulation result for  $^{182}\text{Ta}$  is shown in Fig.4, where only the energy deposition is displayed (the experimental Gaussian broadening is not taken into account). In this low-energy spectrum, one can observe the peaks characteristic of the  $^{182}\text{Ta}$  decay (gamma emissions and X-ray emissions from tungsten) as well as the peaks (in red) corresponding to the induced niobium fluorescence.

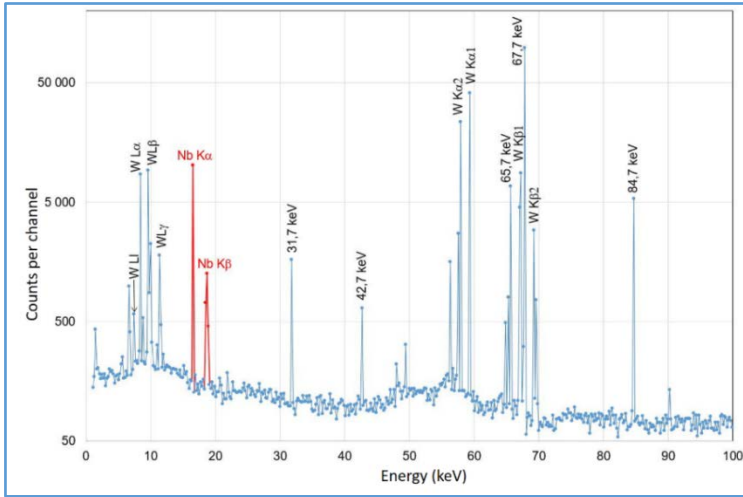


**Fig. 4.** Simulated spectrum following the decay of  $^{182}\text{Ta}$  in a niobium dosimeter

The correction factor for the niobium K X-ray peak with energy  $E$ , is the number of events corresponding to this energy (the channel content minus the background),  $N_p$ , divided by the number of simulated radioactive decays,  $N_T$ , and by the X-ray spectrometer efficiency  $\varepsilon(E)$  (Equation 2):

$$C_N(E) = \frac{1}{\varepsilon(E)} \cdot \frac{N_p}{N_T} \quad (2)$$

The correction factor was calculated for each of the niobium  $\text{XK}\alpha$  and  $\text{XK}\beta$  peaks and is expressed in  $\text{s}^{-1} \cdot \text{Bq}^{-1}$ ; it corresponds to the number of X rays emitted per decay of the specific radioactive impurity. Therefore, it must be multiplied by the activity of the impurity and the detection efficiency to determine the spurious fluorescence count rate that must be subtracted from the net area of the full-energy peak. The correction factors for the different impurities are presented in Table 2; typical relative uncertainties are 1 % for the  $\text{K}\alpha$  corrective factors and 3 % for the  $\text{K}\beta$  ones.

**Table 2.** Correction factors for fluorescence induced by gamma-emitting impurities

Radionuclide	Corrective factor for $\text{K}\alpha$ ( $\text{s}^{-1} \cdot \text{Bq}^{-1}$ )	Corrective factor for $\text{K}\beta$ ( $\text{s}^{-1} \cdot \text{Bq}^{-1}$ )
$^{92\text{m}}\text{Nb}$	$1.489 \cdot 10^{-4}$	$2.198 \cdot 10^{-5}$
$^{94}\text{Nb}$	$1.003 \cdot 10^{-2}$	$1.85 \cdot 10^{-3}$
$^{95}\text{Nb}$	$2.55 \cdot 10^{-3}$	$5.5 \cdot 10^{-4}$
$^{95\text{m}}\text{Nb}$	0.364	0.0712
$^{182}\text{Ta}$	$5.42 \cdot 10^{-2}$	$1.05 \cdot 10^{-2}$
$^{183}\text{Ta}$	$8.21 \cdot 10^{-2}$	$1.48 \cdot 10^{-2}$

This study allows deriving some general remarks on the importance of the impurities:

- i. The influence of  $^{92m}\text{Nb}$  is very small, as it emits mainly energetic photons (934 keV); the K X-rays of zirconium are well separated on the spectra and are therefore not considered here.
- ii. Both  $^{94}\text{Nb}$  and  $^{95}\text{Nb}$  emit K X-rays from molybdenum; since the energy of the molybdenum  $\text{XK}\beta$  (19.62 keV) is just above the niobium K ionization threshold (18.98 keV), it has a high probability of photoelectric interaction in the dosimeter material and thus of generating the niobium fluorescence. However, the low intensity of Mo K X-rays emissions (about 0.2 % and 0.01 % for  $^{94}\text{Nb}$  and  $^{95}\text{Nb}$  respectively) limits their contribution.
- iii. The effect of  $^{95m}\text{Nb}$  is reflected both by the fluorescence induced by 200 keV photons and especially by the direct emission of K X-rays from niobium, leading to a large correction factor, but in many cases,  $^{95m}\text{Nb}$  can be allowed to decay.
- iv. The correction factors for  $^{182}\text{Ta}$  and  $^{183}\text{Ta}$  are of the same order of magnitude, the fluorescence being mainly induced by the K X-rays lines of tungsten.

In addition, with the information on the process responsible for the niobium ionization, it was shown that electrons are mainly responsible for the fluorescence effects in niobium dosimeters [8].

## 4 Experimental validation

To validate the calculated correction factors, these were applied to nine dosimeters (3 strips and 6 discs) with three impurity levels (0.3 ppm, 4 ppm and 19.6 ppm). These dosimeters were measured six times throughout the year following the end of the irradiation using gamma- and X-ray spectrometry to determine respectively the impurities activity and the Nb X-rays emission rates. These counting rates were corrected for the impurities contribution using the calculated correction before deriving the  $^{93m}\text{Nb}$  activity at the same reference date. It must be noted that the very short-lived impurities ( $^{95m}\text{Nb}$  and  $^{183}\text{Ta}$ ) were not taken into account and that  $^{92m}\text{Nb}$  only appears in the first series of measurements. Figure 5 shows the one-year evolution of the raw and corrected values for three among the six disc dosimeters.

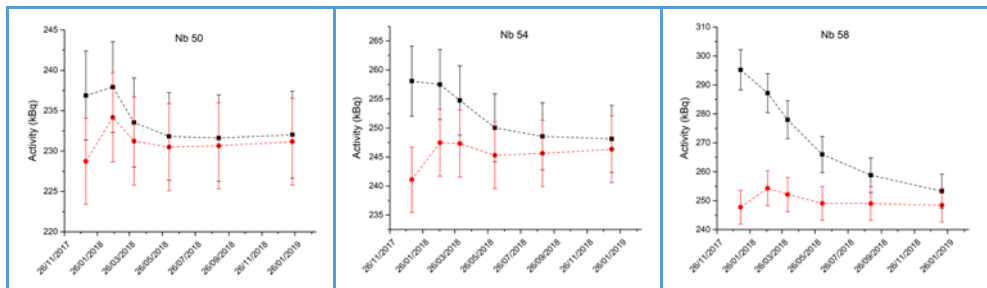


**Fig. 5.** Activity of  $^{93m}\text{Nb}$  at the reference date for 3 discs without (black) and with (red) correction of the fluorescence of impurities (Ta impurities 0.3, 4 and 19.6 ppm)

In figure 5, the red curves of the activities obtained after application of the calculated correction coefficients are almost flat and thus show the relevance of the application of these coefficients, to obtain, whatever the cooling duration and the importance of the initial deviation, a reliable value of activity. These results are summarized in Table 3 that presents the mean values obtained during the six series of measurements, and compares the raw activity values (column 3) with the fluorescence-corrected values (column 6). The individual activities are obtained with a relative standard uncertainty of about 2.3 %. Maximum

fluorescence correction factors (at the reference date) range from a few percent (3.5 %) for the 0.4 ppm Ta samples to about 17 % for the 19.6 ppm ones. It can be seen that taking into account the fluorescence corrections leads to consistent activity values at each measurement date: the standard deviation between the six measurements is reduced to about 1 %. At the same time, the mean value of the six results is significantly reduced, by up to 10 % for dosimeters containing a high proportion of tantalum.

**Table 3.** Mean activity values and associated standard deviation (SD) without and with fluorescence corrective factors, and relative differences between these.

Dosimeter number	Ta (ppm)	Mean raw activity (R) (kBq)	SD (kBq)	Relative SD (%)	Mean corrected activity (C) (kBq)	SD (kBq)	Relative SD (%)	Relative difference (C-R)/R*100 (%)
Nb8 (S)	0.3	23.28	0.26	1.11	<b>22.86</b>	<b>0.45</b>	<b>1.98</b>	<b>-1.84</b>
Nb17 (S)	4	34.84	0.77	2.22	<b>33.88</b>	<b>0.42</b>	<b>1.23</b>	<b>-2.83</b>
Nb26 (S)	19.6	27.48	1.56	5.67	<b>25.39</b>	<b>0.40</b>	<b>1.90</b>	<b>-8.23</b>
Nb49 (D)	0.3	232.23	1.26	0.54	<b>229.35</b>	<b>2.68</b>	<b>1.17</b>	<b>-1.26</b>
Nb50 (D)	0.3	233.97	2.77	1.18	<b>231.08</b>	<b>1.77</b>	<b>0.77</b>	<b>-1.25</b>
Nb53 (D)	4	255.30	5.93	2.32	<b>247.88</b>	<b>0.74</b>	<b>0.30</b>	<b>-2.99</b>
Nb54 (D)	4	252.84	4.50	1.78	<b>245.52</b>	<b>2.34</b>	<b>0.95</b>	<b>-2.98</b>
Nb57 (D)	19.6	255.77	14.52	5.68	<b>234.33</b>	<b>1.31</b>	<b>0.56</b>	<b>-9.15</b>
Nb58 (D)	19.6	273.08	16.47	6.03	<b>250.13</b>	<b>2.55</b>	<b>1.02</b>	<b>-9.18</b>

## 5. Conclusion

The methodology based on Monte Carlo simulations to calculate fluorescence effects has been successfully applied to correct X-ray peaks areas from nine niobium dosimeters with different level of tantalum impurities. The fluorescence correction factors determined by calculation were applied to these irradiated dosimeters and allowed to obtain consistent results between the different measurements carried out over a one-year period. It can be concluded that, using this approach, it is possible to perform reliable measurements by X-ray spectrometry shortly after the activation date. However, it must be noted that the correction factors are geometry dependant (dosimeter thickness and composition, detection efficiency), therefore specific correction factors should be computed for each experimental condition.

## References

1. ASTM E1297, Standard Test Method for Measuring Fast-Neutron Reaction Rates by Radioactivation of Niobium (2018)
2. D. Thornton *et al.*, The Second EWGRD Round Robin: Inter-Comparison of  $^{93m}\text{Nb}$  Measurements (this conference)
3. IAEA. ENDF: Evaluated Nuclear Data File, <http://www-nds.ciae.ac.cn/exfor/endl.htm> (2018)
4. DDEP, [http://www.lnhb.fr/ddep\\_wg/](http://www.lnhb.fr/ddep_wg/) (2022)
5. M.-C. Lépy, A. Pearce and O. Sima, *Metrologia* 52, S12-145 (2015), <http://dx.doi.org/10.1088/0026-1394/52/3/S123>
6. Y. Ménesguen, M.-C. Lépy, *Nucl. Instrum. Methods Phys. Res. A*, 1003, 165341 (2021), <https://doi.org/10.1016/j.nima.2021.165341>

7. F. Piton, M.-C. Lépy, M.-M. Bé, J. Plagnard, *Appl. Radiat. Isot.*, **52**, 791-795 (2000), [https://doi.org/10.1016/S0969-8043\(99\)00246-8](https://doi.org/10.1016/S0969-8043(99)00246-8)
8. J. Riffaud, PhD thesis, Université Paris-Saclay (2018)
9. E. García-Toraño, V. Peyrés, M.-M. Bé, C. Dulieu, M.-C. Lépy, and F. Salvat., *Nucl. Instrum. Methods Phys. Res. B*, **396**, 43-49 (2017)
10. S. Agostinelli, *Nucl. Instrum. Methods Phys. Res. A*, **506**, 250–303 (2003)
11. F. Salvat, *PENELOPE-2018: A code System for Monte Carlo Simulation of Electron and Photon Transport*, Document NEA/MBDAV/R(2019)1, OECD Nuclear Energy Agency, Boulogne-Billancourt, France, 2019. Available from <http://www.nea.fr/lists/penelope.html>.